Supporting Information

Fiebiger et al. 10.1073/pnas.1505292112

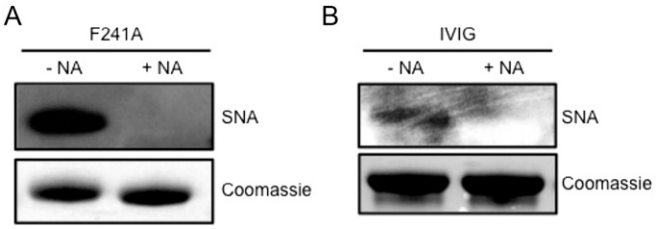

Fig. S1. Verification of sialic acid contents by Sambucus nigra (SNA) lectin blotting. Preparations of F241A (*A*) and IVIG (*B*) were detected with SNA by Western blotting to analyze their sialic acid contents. The respective bands in the Coomassie stain served as loading controls.

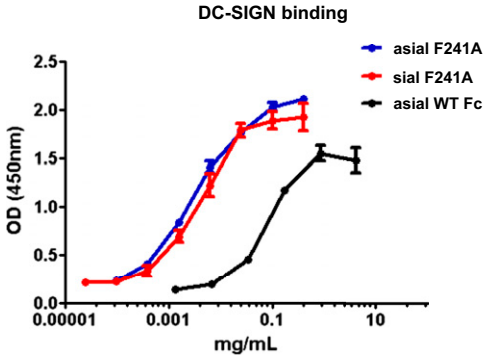

Fig. S2. F241A binds to DC-SIGN independent of sialylation. Recombinant DC-SIGN was immobilized, and binding affinity of asialylated (asial F241A), sialylated F241A (sial F241A), and asialylated wild-type Fc (asial WT Fc) was measured by ELISA. Means ± SEM are plotted.

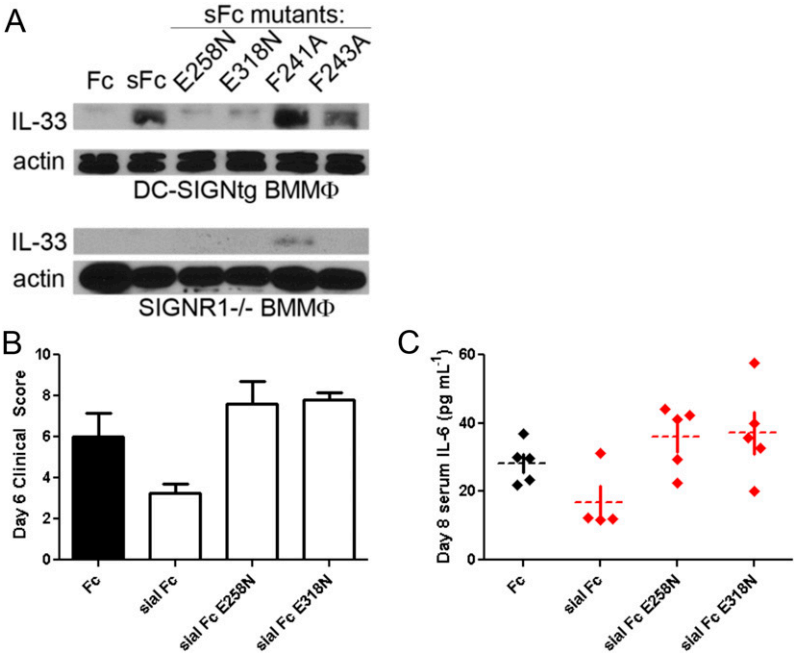

Fig. S3. E318/Lys340 pocket is critical for the antiinflammatory effect of sialylated Fc. (*A*) Bone marrow cells from SIGN-R1$^{-/-}$ and hDC-SIGN^{+} (DC-SIGNtg) mice were isolated and differentiated in vitro into bone marrow-derived macrophages (BMMΦs). BMMΦs were pulsed with wild-type or mutant Fc. Whole-cell extracts were used for Western blotting. Actin served as loading control. (*B*) K/BxN-challenged C57BL/6 mice were treated with different Fc preparations. Clinical scores of disease were monitored on day 6 posttreatment. Means ± SEM are plotted. (*C*) Serum IL-6 levels were tested by ELISA 8 d posttreatment.

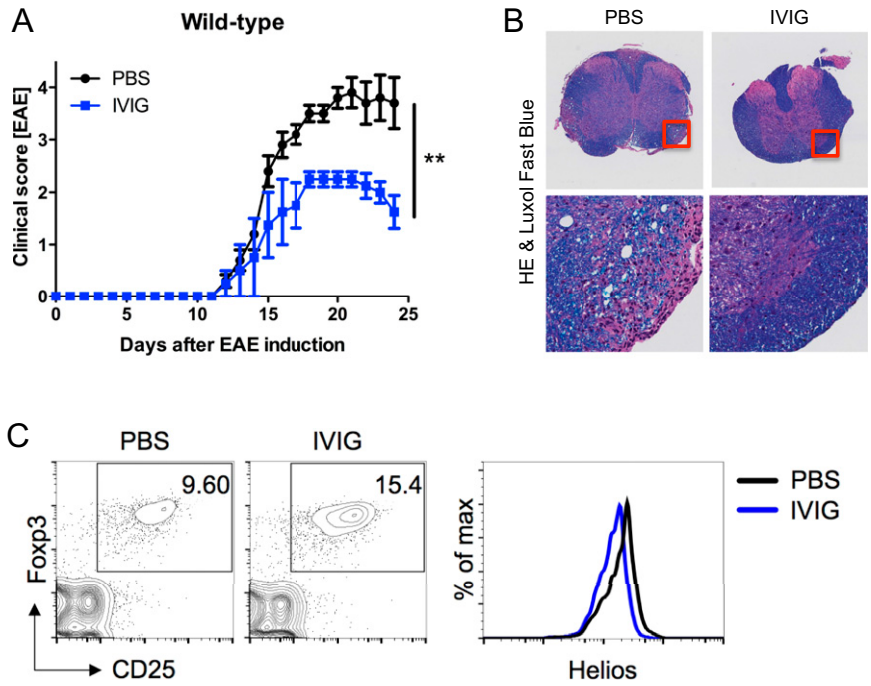

Fig. S4. IVIG selectively expands inducible T_{reg} cells. EAE was induced in C57BL/6 wild-type mice by immunization with $MOG_{35–55}$ peptide emulsified in CFA. Mice were treated with PBS or IVIG (1 g/kg). (*A*) Clinical scores of EAE are depicted. Means ± SEM are plotted; $^{**}P < 0.01$ determined by Tukey's post hoc test. (*B*) Representative images of hematoxylin and eosin (HE) and Luxol Fast Blue staining of spinal cords from EAE mice. HE stains for inflammation. Loss of signal in Luxol Fast Blue staining reflects progressed demyelination. (*Lower*) Magnification of areas boxed in red (*Upper*). (*C*) Cells from draining lymph nodes were isolated and analyzed for T_{reg}-cell numbers and their expression of the nT_{reg}-specific transcription factor Helios.

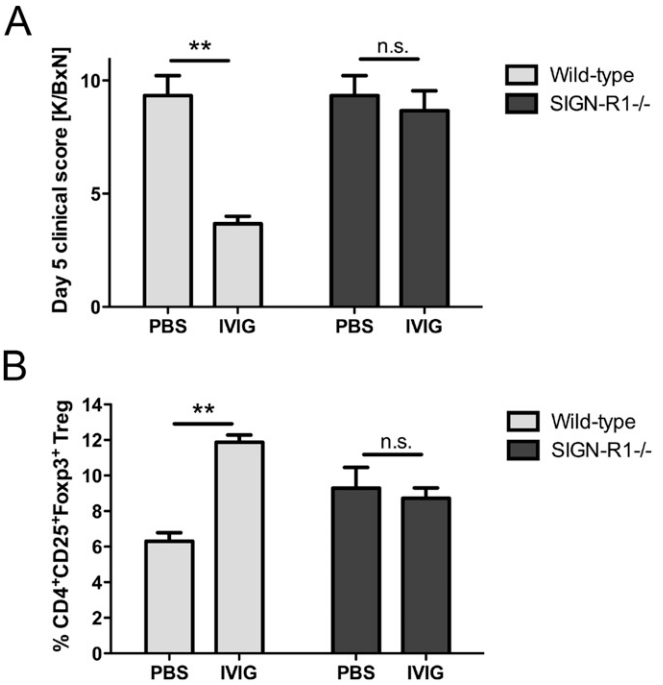

Fig. S5. Loss of SIGN-R1 abrogates the positive effect of IVIG on T_{reg} cells. C57BL/6 wild-type and SIGN-$R1^{-/-}$ mice were given IVIG (1 g/kg) or PBS intravenously. One hour later, mice were challenged with K/BxN serum. (*A*) Clinical signs of arthritic disease were monitored 5 d after challenge. (*B*) T_{reg} cells from spleens were analyzed by flow cytometry. Means ± SEM are plotted; $^{**}P < 0.01$ determined by Student's *t* test. n.s., not significant.

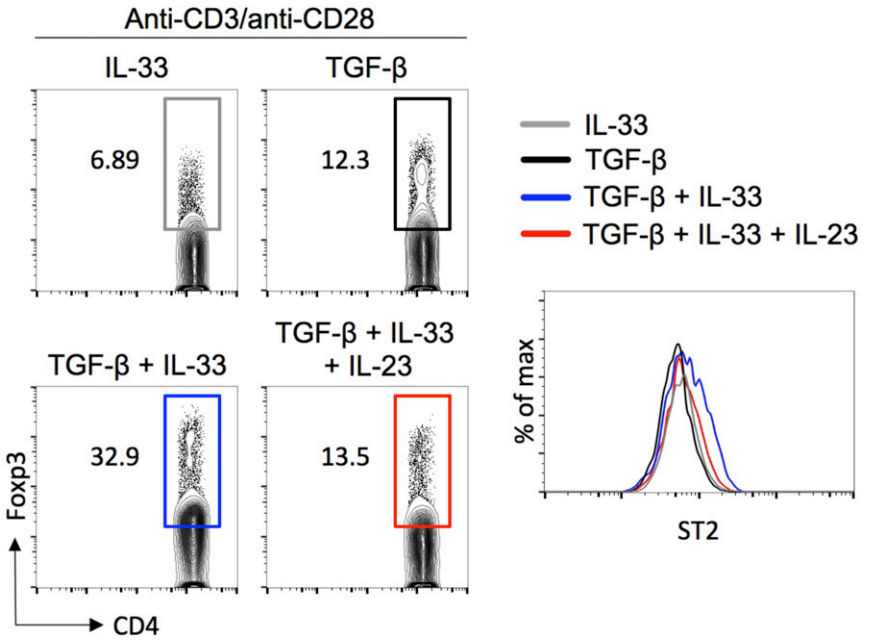

Fig. S6. IL-33 synergistically contributes to T_{reg}-cell differentiation in vitro. Naïve $CD4^+$ T cells were isolated from spleens of C57BL/6 wild-type mice. Cells were cultured 3 d in the presence of anti-CD3/CD28. To drive T_{reg}-cell differentiation, TGF-β was added to the cells either alone or in combination with IL-33 and IL-23. T_{reg}-cell numbers and ST2 expression were analyzed by flow cytometry.

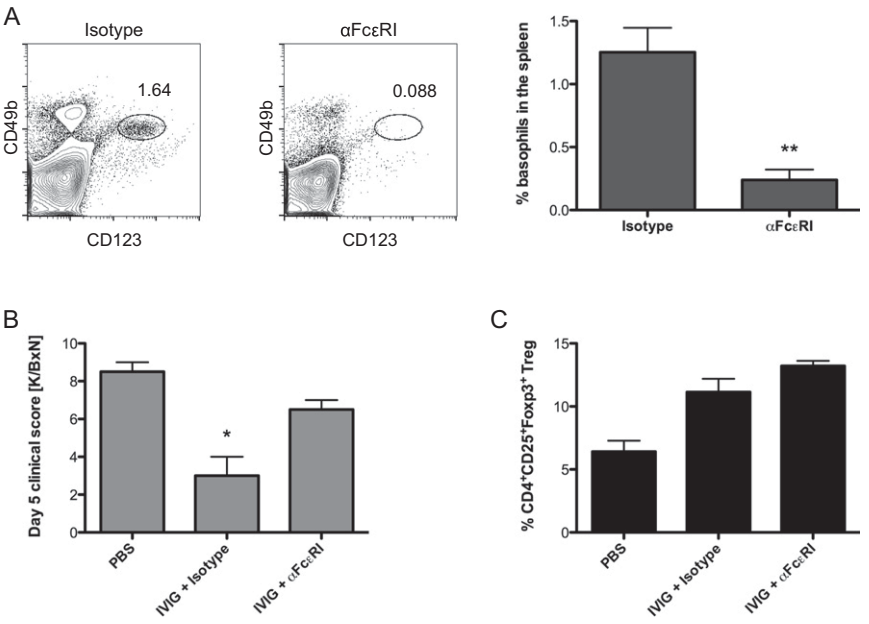

Fig. S7. Basophil depletion does not affect IVIG-mediated T_{reg}-cell stimulation. C57BL/6 wild-type mice were treated with anti-FcεRI antibody to deplete basophils or with an isotype control. In addition, mice received IVIG (1 g/kg) or PBS and were challenged with K/BxN sera. (*A*) FACS analysis of splenic basophils 5 d after injection. (*B*) Clinical signs of arthritic disease were monitored on day 5 post disease induction. (*C*) Splenic T_{reg} cells were analyzed by flow cytometry. Means ± SEM are plotted; $*P < 0.05$; $**P < 0.01$ determined by Tukey's post hoc test.

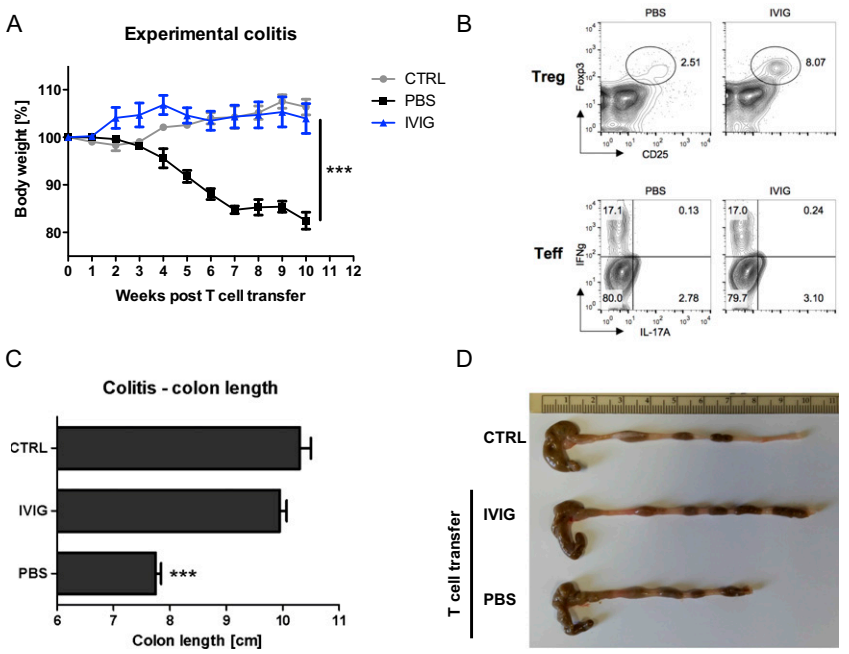

Fig. S8. IVIG preferentially activates iT_{reg} cells and protects from experimental colitis. C57BL/6 $Rag1^{-/-}$ mice were injected with $CD4^{+}CD45RB^{high}CD25^{-}$ T cells to induce T-cell transfer colitis. Mice were treated once a week with PBS or IVIG (1 g/kg) starting 4 wk post T-cell transfer. $Rag1^{-/-}$ control mice (CTRL) did not receive any T cells. (*A*) Body weight was measured once a week. Body weight loss was used as a measure of disease severity. (*B*) Cells from draining lymph nodes were analyzed for percentages of T_{reg} cells and $CD4^{+}$ effector T cells by FACS. (*C*) Entire colons were dissected and measured. Colon shrinkage reflected disease severity and correlated with body weight loss. (*D*) Representative image of dissected colons as described in *C*. Means ± SEM are plotted; ***$P < 0.001$ determined by Tukey's post hoc test.

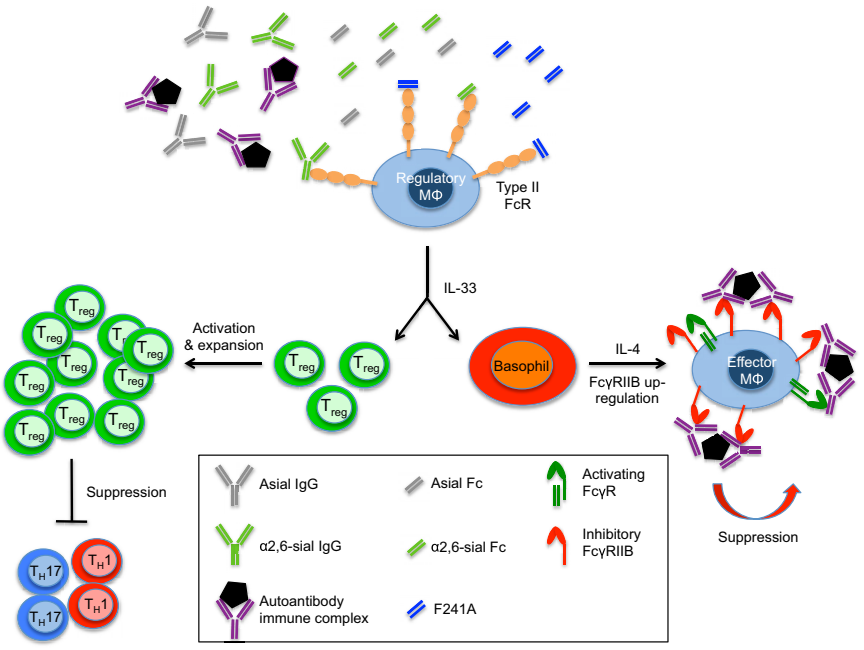

Fig. S9. Proposed model of sFc-induced antiinflammatory pathways. Sialylated IgG (sFc) as well as the sialylated Fc analog F241A selectively engage type II FcRs such as SIGN-R1 or human DC-SIGN on regulatory macrophages and induce IL-33 production. IL-33 is a central mediator that induces two different antiinflammatory pathways. Basophils respond to IL-33 with production of IL-4, which in turn induces the up-regulation of the inhibitory FcγRIIB on effector macrophages. The resulting dramatic change of their activation threshold suppresses inflammation. In addition, IL-33 also triggers activation and expansion of T_{reg} cells, which effectively suppress T_H1 and T_H17 cells, thus ameliorating T cell-mediated autoimmunity.